

Surface roughness and alloy stability interdependence in lattice-matched and lattice-mismatched heteroepitaxy

Catherine Priester and Genevieve Grenet

IEMN, Département ISEN, CNRS-UMR 8520, Boîte Postale 69 F-59652, Villeneuve d'Ascq Cedex, France

Ecole Centrale de Lyon, LEOM, CNRS-UMR 5512, Boîte Postale 163 F-69131, Ecully Cedex, France

(Received 16 September 1999)

How the possibility of a better strain relaxation introduced by the surface roughness can modify alloy demixing is investigated here. We propose a step-by-step model to simulate the growth process on a rough surface. We use an atomistic description and also consider the surface tension difference between the two binaries that form the ternary alloy. This study clearly shows how and why—in the lattice-matched case—the atoms corresponding to the binary materials with the lowest surface tension naturally tends to segregate towards initially sloping areas, whereas—in the mismatched case—upper areas are enriched in the more strained binary. The results are exemplified by $\text{Al}_{0.5}\text{In}_{0.5}\text{As}$ lattice matched or not to its substrate. Throughout this article, we discuss the balance among mixing enthalpy, strains, and the difference of surface tension between the two binaries that form the ternary alloy.

I. INTRODUCTION

Partial alloy demixing is a well-known phenomenon¹⁻⁴ for most III-V alloys (whether lattice matched or not to the substrate) such as $\text{Al}_x\text{In}_{1-x}\text{As}$ or $\text{Ga}_x\text{In}_{1-x}\text{P}$ when grown by molecular beam epitaxy (MBE). This leads to composition modulations parallel and perpendicular to the growth surface. Understanding this phenomenon is very important as it can strongly modify the optical and electronic properties of the resulting material (e.g., depending on whether the alloy demixes or not, one obtains either a semi-insulant or a semiconductor). Let us first emphasize the fact that here we shall *not consider spinodal decomposition*, which is viewed as a bulk phenomenon, *but alloy demixing, which occurs only on the growth front and is frozen as growth continues*.

On the one hand, for alloys that are lattice matched to their substrate, we have already shown that such demixing is strictly forbidden if the surface is ideally flat.⁵ However, a growth front is never ideally flat and always presents some intrinsic surface roughness. In this case, it could be energetically favorable to increase this roughness (even if the surface energy concurrently increases) in order to decrease the alloy mixing enthalpy contribution to the total energy.⁶ On the other hand, it is now well established that when a material is stressed because it is coherently deposited on a substrate with a different lattice parameter, its total energy can also be lowered by a roughening of its surface.⁷ It follows that, if the material is now an immiscible stressed alloy, the latter surface instability (mismatch induced) strongly interacts with the former surface instability (alloy demixing induced) because both are elastic effects in nature.⁸ In both cases, the surface energy usually concurrently increases. However, the surface energy itself can depend both on alloy decomposition (because of the propensity of alloys to lower their surface energy by segregating the most adequate binary towards the surface) and on mismatch stresses. In summary, it appears that for immiscible alloys (matched or not to the substrate), there exists a complex interdependence between phase separation,

surface morphology, and mismatch stresses.

In this regard, several authors have already studied some aspects of the problem. Reference 9 focuses on the effect of stress on phase separation during step flow growth using the continuous elasticity theory. Reference 10 concentrates on the coupling between phase separation, strain relaxation, and morphological instability. Reference 11 also studies the phase and surface stability for a static or growing immiscible alloy. However, no attempt has been made yet to describe the deposition of strained immiscible material using a microscopic model such as the Keating model used here in which the growth process is simulated by a monolayer-by-monolayer model.

In the present paper, we summarize the information we collected from the study of numerous growth simulations for matched or mismatched alloys deposited on substrates of different roughnesses. The paper is organized as follows. First, we will present the key features and limits of the model used. Then, we will investigate alloy decomposition as a function of the surface morphology, viz., made of either islands or pits, in the case of lattice-matched immiscible alloys. And finally, we will study how this alloy demixing is modified when the alloy is no longer lattice matched to its substrate. Throughout this paper, results are exemplified by the case of $\text{Al}_x\text{In}_{1-x}\text{As}(001)$.

II. THE MODEL USED AND ITS KEY FEATURES

A. A typical immiscible III-V semiconductor alloy: $\text{Al}_x\text{In}_{1-x}\text{As}$

Most of the III-V ternary semiconductor alloys $A_{1-x}B_xC$ may be seen as pseudobinary compounds $(AC)_{1-x}(BC)_x$ with x ranging from 0 to 1. The A and B atom distribution on the zinc blende lattice may or may not present deviation from complete randomness. The alloy propensity to bulk phase separation is usually quantified with a parameter Ω called the interaction coefficient, the mixing enthalpy being approximately given by $x(1-x)\Omega$. Note that this interaction parameter Ω can be accurately calculated from the Keating

model used in this paper.⁵ To illustrate our purpose, we have chosen the academic case of $(\text{AlAs})_{1-x}(\text{InAs})_x$ (common anion, different cation) with $x=0.5$, which corresponds to the mixing enthalpy maximum. In fact, the choice can be considered to illustrate III-V semiconductors well because (i) the $\text{Al}_x\text{In}_{1-x}\text{As}$ interaction coefficient $\Omega = 3600$ cal/mole is in the middle range for III-V semiconductors between that of $\text{Ga}_x\text{In}_{1-x}\text{As}$ ($\Omega = 2490$ cal/mole) and that of $\text{Ga}_x\text{In}_{1-x}\text{P}$ ($\Omega = 4560$ cal/mole) (Ref. 12) and (ii) the composition 0.5 is close to the value ($x=0.52$) corresponding to the lattice matching of $\text{Al}_x\text{In}_{1-x}\text{As}$ on InP. Furthermore, because we want to disconnect strain effects from composition effects, we chose to keep this alloy concentration constant when investigating the 2% lattice-mismatching effect, a 2% mismatching being considered the limit between strong and weak stresses. Finally, the difference in surface tension (which is related to the difference in the dangling bond) between the two binaries (InAs and AlAs) that form the ternary alloy $\text{In}_x\text{Al}_{1-x}\text{As}$ has also been included in the calculation as an input parameter. For the $\text{In}_x\text{Al}_{1-x}\text{As}$ case, InAs surface tension is lower than AlAs surface tension¹³ (by typically 3–400 meV, but the result depends only on the qualitative value of this quantity) and thus In atoms will naturally segregate toward the surface.¹⁴ In others words, this means that the surface energy itself depends on alloy decomposition because of this propensity of alloys to lower their surface energy by segregating the most adequate binary towards the surface. From this actual example, one can see that the driving impetus for phase separation comes from a combination of mixing enthalpy effect (intrinsic strain effect), mismatch strain effect (extrinsic strain effect), and complex growth front morphology and energy requirements.

B. Growth front morphology modeling

In the present study, for the sake of simplicity we will separately consider two types of surface roughness either made up of 2–3 monolayers (ML's) of platelets (as considered in Ref. 6) or made up of 2–3 ML rectangular shaped holes. We will consider periodic systems with two bumps or two holes per period, so that we do not impose the same periodicity for alloy decomposition and for surface roughness. This type of surface morphology is thought to describe a growth front morphology well, even for strained material but below the bidimensional-to-tridimensional growth transition. In the present model indeed, the effect of strain on phase demixing is taken into account but not the effect of strain on morphology, the latter being simply injected into the model and kept in two dimensions. The facet orientations are taken to be rather flat, i.e., $[11\bar{3}]$ orientations as experimentally observed. In order to emphasize the mechanisms involved, we have chosen to model the systems with platelets (holes) that present wide enough flat tops (bottoms), so that one can separate what we will refer to below as *flat areas* (top and/or bottom areas) from *sloping areas* (facet areas). We will also distinguish in the following *upper areas* (tops of platelets and tops of spaces between holes) from *lower areas* (bottoms of holes and bottoms of spaces between platelets).

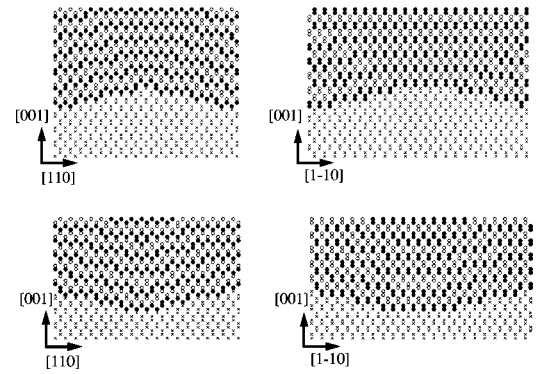


FIG. 1. Cross-section views of the successive snapshots modeling growth on a rough surface. (a) and (b): surface that shows bumps; (c) and (d): surface that shows pits. Cross-section planes are $[110]$ (a and c) and $[1\bar{1}0]$ (b and d). Filled squares and open circles represent atoms deposited in successive steps. The present initial roughness is made up of 3 monolayers.

C. Growth front modeling

The most important point to be noted is thus that the final result is closely bound to the way the growth front morphology and progress will be simulated. Because in MBE growth at the usual growth temperature, bulk diffusion is negligible, the only cations allowed to exchange in the present model⁶ belong to the 2 upper ML's (viz., the surface layer and the layer just underlying it). For details see Ref. 6. To model the growth process itself, we have chosen to capture a sequence of snapshots. Between two consecutive snapshots, about 1 ML of random alloy has been deposited on the surface. Moreover, we suppose that all surface atoms are able to exchange, this means that the growth conditions (not too high growth rates and not too low growth temperature) keep the process safe from kinetic limitations. One has also to remember that, due to surface tension requirements, and as the growth orientation is $[001]$, III-V surfaces must be dimerized^{15,16} at any step of the growth process. Let us first show in Fig. 1 how this criterion “surfaces must be dimerized” induces a difference between growth on bumps and on holes. In the case of bumps, the deposited ML results from covering every anion surface atom with entities made of an anion dimer and its four underlying cations. This means that when we move from one step to the next in the growth sequence, the platelet that defines the roughness enlarges by one atom along the $[110]$ direction and by two atoms along the $[1\bar{1}0]$ dimers direction (as can be viewed in Fig. 1). In the case of pits, as the edges are concave, the criterion “surfaces must be dimerized” is verified more simply, so that when we move from one step to the next, the pit that defines the roughness narrows by one atom along both $[110]$ and $[1\bar{1}0]$ directions. One consequence of this growth process modelling is that after the deposition of several ML's (the number depends on the starting point of the sequence), the roughness disappears and a flat surface on which new roughness may develop is recovered. It is clear that our purpose here is not to fully describe the surface flatness recovery [because we are concerned with a two-dimensional (2D) growth mode] but rather to emphasise what happens when a 2D surface is rough enough to allow surface demixing.

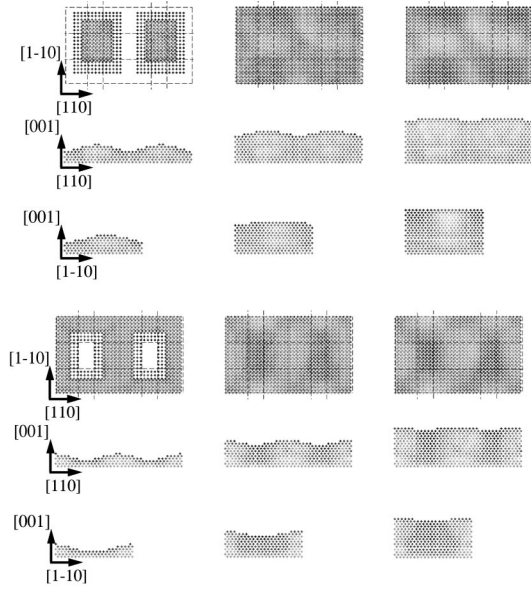


FIG. 2. Lattice-matched case: Successive top and cross-section views of growth on a rough surface with bumps (a) and pits (b) (from 0, 5, and 10 deposited monolayers); the alloy is lattice-matched to the substrate. Indium-rich atomic rows correspond to darker symbols and Al-rich rows to brighter symbols.

III. RESULTS AND DISCUSSION

All our “alloy decomposition” results are collected in Fig. 2 for lattice-matched growth, in Fig. 3 for compressively strained growth, and in Fig. 4 for tensilely strained growth. In these figures, each full circle corresponds to an atomic row (cations) and the gray level indicates the average of the local concentration (for each cation the local concentration over the cation and its 12 first cation neighbors is calculated). For top views, the local concentration is averaged over the

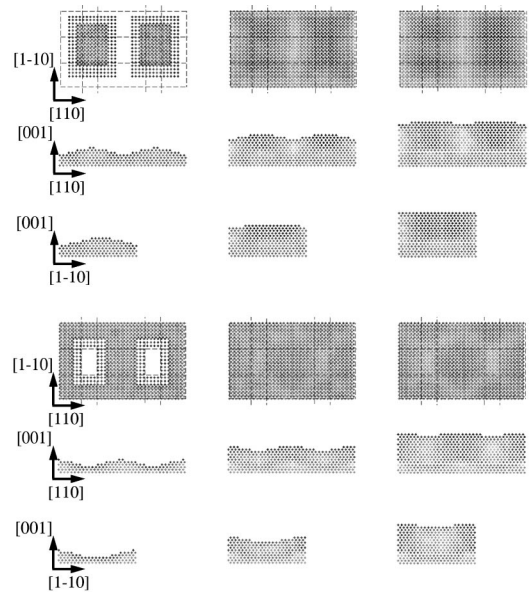


FIG. 3. Compression case: Successive top and cross-section views of growth on a rough surface with bumps (a) and pits (b) (from 0, 5, and 10 deposited monolayers); the substrate forces the alloy to be in compression. Indium-rich atomic rows correspond to darker symbols and Al-rich rows to brighter symbols.

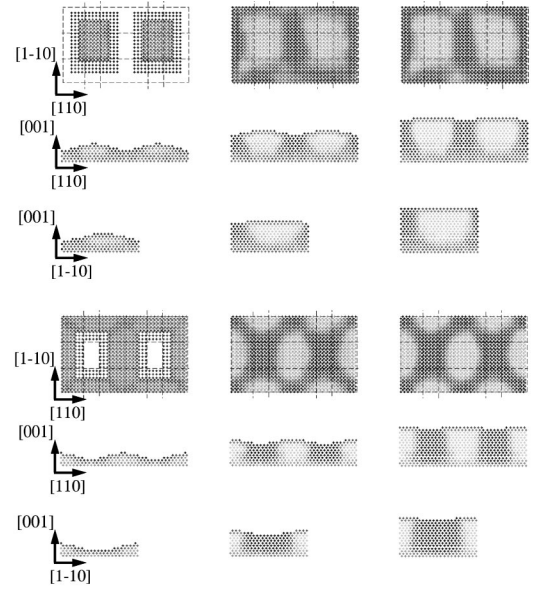


FIG. 4. Tension case: Successive top and cross-section views of growth on a rough surface with bumps (a) and pits (b) (from 0, 5, and 10 deposited monolayers); the substrate forces the alloy to be in tension. Indium-rich atomic rows correspond to darker symbols and Al-rich rows to brighter symbols.

whole row above the substrate, whereas for cross sections it is averaged over the slice in between the parallel dashed lines on top views. This way, the first glance at the figures gives a global idea of the alloy decomposition in the system. Dark areas correspond to In-rich zones and bright areas to Al-rich zones. Figures 2 to 4 correspond to a chosen typical initial rough morphology, but several other systems (with various period sizes, depths of roughness, and mismatches) have been calculated, leading to results that corroborate those described below.

A. Lattice-matched alloy case

For the $\text{In}_x\text{Al}_{1-x}\text{As}$ case, as InAs surface tension is lower than AlAs surface tension,¹³ In atoms (which are larger than Al atoms) segregate toward the surface. This is the main explanation for what can be observed for the lattice-matched case (Fig. 2): for the two cases of surface roughness (made up of pits or bumps), the aluminum-rich areas (bright zones) correspond to those areas that remain flat during the growth simulation, whereas the indium-rich areas correspond to the location of sides as more and more layers are deposited (i.e. sloping areas). We have checked that if we artificially change the sign of surface tension difference, we get exactly the opposite situation. This demonstrates that surface tension is the key parameter for such systems. This also indicates that the use of a surfactant can strongly modify alloy decomposition. It is interesting to note the strong non equivalence of the $[110]$ and $[1\bar{1}0]$ directions in the case of bumps, which can be related to the change of slope due to dimer surface requirements. In a previous study⁶ limited to very short period bumpy systems, we had concluded that the bumps were In enriched. This was due to the fact that the bumps were so small that there was no flat area on top of them, so bumps were only made up of sloping areas.

B. Mismatched (tension and compression) alloy cases

If the deposited alloy is no longer lattice matched to its substrate, previous experimental^{17,18} and theoretical¹⁹ studies have demonstrated that, in the case of *dots*, the strain, combined with surface effects, favors alloy decomposition for compressively strained film. By studying Figs. 3 and 4, information can be obtained on what happens in the case of *slight roughness*. Figure 3 clearly displays In enrichment in the upper areas whereas Fig. 4 shows Al enrichment in these same upper areas. This indicates that the segregation zones due to the strain effect (upper and lower areas) are different in nature from the segregation zones due to the surface tension effect (flat and sloping areas). From this one can deduce that in general, it is not possible to take advantage of strain for counterbalancing the segregation action of the surface tension. However, from Figs. 3 and 4 one can also see, contrary to what is generally assumed, that (i) 2% mismatching can be strong enough for overcoming the effect of surface tension and (ii) larger atoms (In) do not necessarily segregate toward upper areas or edges (as clearly evidenced in Fig. 4). The general rule for alloy demixing on rough strained layer surfaces can be stated as follows: *the atoms of the binary, which is more strained by the substrate, segregate toward the upper areas*. For $\text{In}_x\text{Al}_{1-x}\text{As}$ in compression, InAs is more strained than AlAs, and this is the opposite for $\text{In}_x\text{Al}_{1-x}\text{As}$ in tension (let us recall here that the alloy concentration remains constant, and we use an academic substrate, moving its lattice parameter). A simple explanation is that the upper areas allow better strain relaxation than lower areas. For intermediate strains (between 0% and 2%) the effect is similar but less marked.

IV. CONCLUDING REMARKS

Let us recall the main features of our study which are summarized in Table I: during the growth of ternary alloys on a rough substrate, when the mismatches between the two binaries and the substrate are of different amplitudes, the ‘‘more strained’’ binary will segregate towards the upper ar-

TABLE I. Summary of In and Al segregation area (sloping, flat, upper or lower) versus morphology (bumps or pits) and alloy strain state (matched, compressive or tensile mismatch).

Morphology	Strain			
		Matched	Compressive	Tensile
Bumps	In	sloping	upper	lower
	Al	flat	lower	upper
Pits	In	sloping	upper	lower
	Al	flat	lower	upper

reas. In the case of equivalently strained binaries, surface effects dominate, and the material with the lower surface tension will segregate towards the sloping area. It is clear that once alloy decomposition has started, roughness will never vanish, but on the contrary it will rather be enhanced. One can thus take advantage of alloy decomposition to favor dot nucleation by making use of a buffer alloy (this has been recently demonstrated for an $\text{InAs}/\text{Al}_x\text{In}_{1-x}\text{As}/\text{InP}$ system compared with on $\text{InAs}/\text{Ga}_x\text{In}_{1-x}\text{As}/\text{InP}$ system.²⁰) Moreover some recent growth experiments on $\text{Ga}_x\text{In}_{1-x}\text{P}/\text{GaP}$ or GaAs can be successfully explained by referring to the general trends we have pointed out here.²¹ Furthermore, in this study we have supposed that all surface atoms are able to exchange; this means that kinetic limitations (not too high growth rates and not too low growth temperature) are not strong enough to forbid exchanges and thus alloy decomposition.²² Conversely, at least for lattice-matched alloy layers, alloy decomposition can be completely halted by entropic disorder when the growth temperature is greater than a critical temperature roughly equal to $\Omega/2R$, R being the perfect gas constant. However, the critical temperature is not the same for a rough or a perfectly flat surface (the roughness indeed enhances the critical temperature).

ACKNOWLEDGMENTS

This work was partly supported by France Telecom (Contract No 96 1B 002). The authors thank Henri Mariette for constructive criticism of the first draft of this manuscript.

¹F. Peiro *et al.*, Appl. Surf. Sci. **65**, 447 (1993).

²O. Ueda *et al.*, J. Cryst. Growth **95**, 38 (1989).

³T. Okada, G.C. Weatherly, and D.W. McComb, J. Appl. Phys. **81**, 2185 (1997).

⁴R.R. Lapiere, T. Okada, B.J. Robinson, D.A. Thompson, and G.C. Weatherly, J. Cryst. Growth **155**, 1 (1995); **158**, 6 (1996).

⁵G. Grenet *et al.*, Appl. Surf. Sci. **123/124**, 324 (1998).

⁶C. Priester and G. Grenet, J. Vac. Sci. Technol. B **16**, 2421 (1998).

⁷R.J. Asaro and W.A. Tiller, Metall. Trans. A **3**, 1789 (1972); M.Y. Grinfeld, Dokl. Akad. Nauk SSSR **283**, 1139 (1985); D.J. Srolovitz, Acta Metall. **37**, 621 (1989).

⁸J.E. Guyer and P.W. Voorhees, Phys. Rev. Lett. **74**, 4031 (1995).

⁹J. Tersoff, Phys. Rev. Lett. **77**, 2017 (1996).

¹⁰F. Glas, Phys. Rev. B **55**, 11 277 (1997).

¹¹F. Leonard and R.C. Desai, Phys. Rev. B **56**, 4955 (1997); **57**, 4805 (1998).

¹²J.L. Martins and A. Zunger, Phys. Rev. B **30**, 6217 (1984).

¹³J.W. Cahn and R.E. Hanneman, Surf. Sci. **1**, 387 (1964).

¹⁴O. Dehaese, X. Wallart, and F. Mollot, Appl. Phys. Lett. **66**, 52 (1995).

¹⁵S.B. Zhang and A. Zunger, Phys. Rev. B **53**, 1343 (1996).

¹⁶S.B. Zhang and A. Zunger, Appl. Phys. Lett. **71**, 677 (1997).

¹⁷N. Grandjean, J. Massies, and O. Tottereau, Phys. Rev. B **55**, R10 189 (1997).

¹⁸A. Rosenauer, U. Fischer, D. Gerthsen, and A. Förster, Appl. Phys. Lett. **71**, 3868 (1997).

¹⁹C. Priester and M. Lannoo, Appl. Surf. Sci. **123/124**, 658 (1998).

²⁰J. Brault, M. Gendry, G. Grenet, G. Hollinger, Y. Desieres, and T. Benyattou, Appl. Phys. Lett. **73**, 2932 (1998); J. Cryst. Growth **201/202**, 1176 (1999).

²¹X. Wallart and F. Mollot, Appl. Surf. Sci. (to be published).

²²J. Tersoff, M.D. Johnson, and B.G. Orr, Phys. Rev. Lett. **78**, 282 (1997).